S3TBX

-

Rayleigh Correction Tutorial

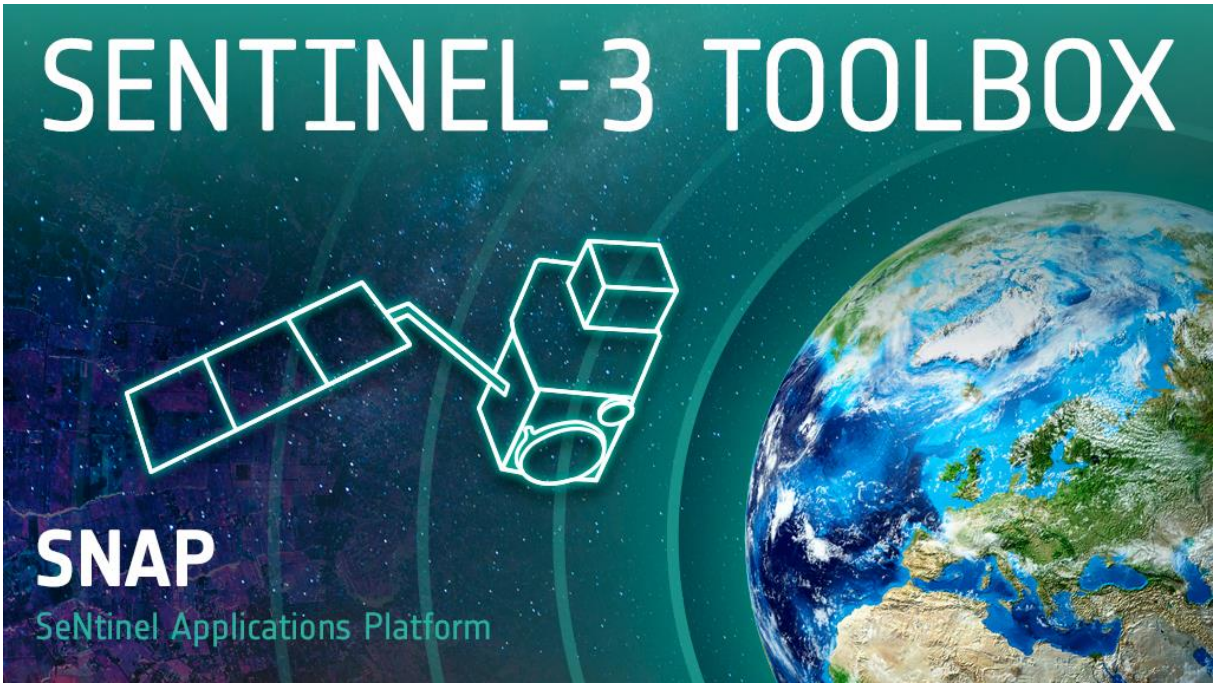

Brockmann Consult GmbH

esa

Authors:	Ana B. Ruescas, Dagmar Müller
Revision	1.0
Date:	11.06.2021

Table of Contents

1. Theoretical background 3
1.1 Scattering by atmospheric gases 4
2. The Rayleigh Correction Processor 9
2.1 Rayleigh Optical Thickness 10
2.2 Bottom of Rayleigh Reflectance 12
2.3 TOA Reflectance Bands 13
2.4 Air Mass 13
3. Example on Sentinel-2 MSI 15
4. References 19

1. THEORETICAL BACKGROUND

Unlike in a vacuum, the atmosphere may affect not only the speed of radiation but also its wavelength, its intensity and its spectral distribution. The four main effects of the atmosphere on the electromagnetic radiation are: refraction, scattering, absorption and reflectance. The combined effects of these factors can reduce the amount of solar radiation reaching the surface.

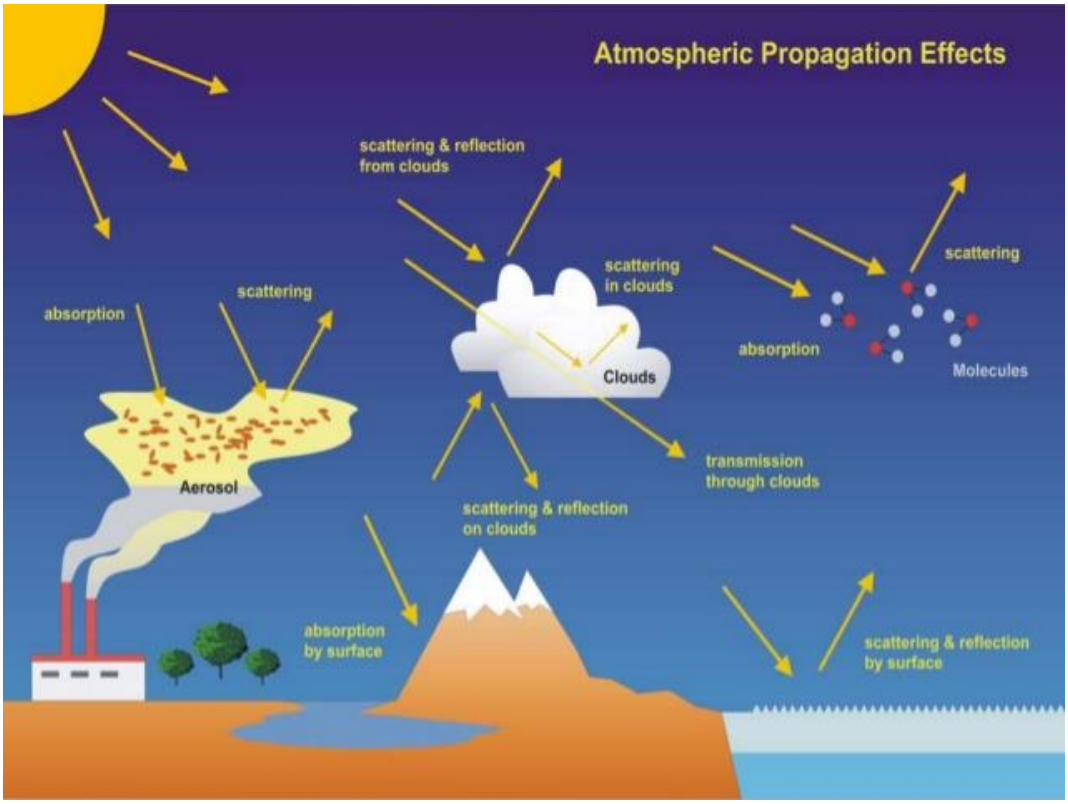

Figure 1 Scheme of the relevant interactions of solar light with the Earth's atmosphere and surface. (Graphics: DLR-IMF)

The radiation field in the atmosphere is commonly characterized by its intensity, which is defined as the flux of energy in a given direction per second per unit wavelength range per unit solid angle per unit area perpendicular to the given direction (Liou, 2002). All interactions between the radiation and the atmosphere are classified either as extinction or as emission. The two processes are distinguished by the sign of the change of the radiation intensity as a result of the interaction. Extinction refers to any process which reduces the intensity in the direction under consideration and therefore includes absorption as well as scattering processes from the original direction into other directions. Emission refers to any process which increases the intensity in the direction under consideration and thus includes scattering into the beam from other directions, as well as thermal or other emission processes within the volume.

Scattering occurs by molecules and various types of aerosols and clouds. Molecular scattering cross-sections are characterised by the Rayleigh (λ^{-4}) law, with aerosol scattering typically showing a much less pronounced dependence on wavelength (about λ^{-1}). Molecular scattering dominates in the UV with aerosols replacing molecules as the major source of scattered light in the VIS and NIR range (see Figure 2).

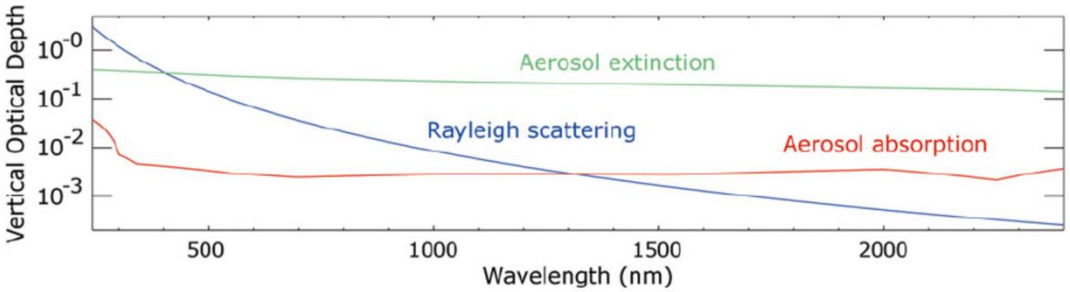

Figure 2. The vertical optical depth due to Rayleigh scattering, aerosol extinction and absorption is given. (Graphics: IUP-IFE, University of Bremen)

1.1 SCATTERING BY ATMOSPHERIC GASES

The molecular scattering consists of two parts: the elastic Rayleigh component which accounts for 96% of scattering events and the 4% inelastic rotational Raman component, which is considered responsible for the so-called Ring effect (filling in of solar Fraunhofer lines in the Earthshine spectra). Differences among types of scattering depending on particle size and wavelength are (Figure 3):

a) **Rayleigh** or molecular scattering occurs when the diameter of the matter is smaller than the wavelength of the incident radiation. The amount of scattering is related to the inverse of the fourth power of the radiation wavelength. Because of its shorter wavelength, blue light is scattered more strongly compared to the red part of the visible spectrum. This process is responsible for the blue colour of the sky.

$\varnothing < \lambda$

Stronger effect at shorter λ (λ^{-4})

b) Mie dispersion or non-molecular dispersion occurs below 4.5 km in the atmosphere, where there are more spherical particles with diameters approximately equal to the size of the wavelength of the incident energy (aerosols, pollution, dust particles, etc.). The size of the particles ranges from 0.1 to 10 times the wavelength. It contributes to the beautiful reddish sunsets.

$\varnothing \approx \lambda$

Clearer effect at longer λ

c) The **non-selective dispersion** takes place in the lower parts of the atmosphere where the particles are larger than 10 times the wavelength of the incident radiation. Here, any wavelength can be scattered equally effectively, hence the clouds appear white, for example.

$\varnothing > \lambda$

Similar at different λ: clouds.

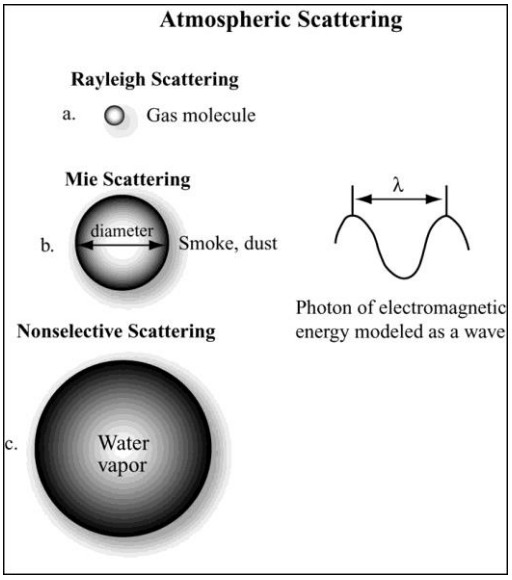

Figure 3. Different types of atmospheric scattering (Source: Jensen, 2009)

In ocean color remote sensing it is important to correct for the effect of the Rayleigh scattering (Figure 4). For a typical open ocean case, for instance with chlorophyll-a concentration of 0.1 mg m−3 and maritime aerosols with aerosol optical thickness of 0.1 at 865 nm, the TOA Rayleigh-scattering radiances contribute about 88%, 83%, 78%, 69%, 59%, and 50% at the

sensor-measured total radiances for the spectral wavelengths at 412, 443, 490, 555, 670, 765, and 865 nm, respectively (Wang, 2016). The radiance contributions from the two near-infrared (NIR) bands are all from atmosphere and ocean surface. If we are able to subtract atmosphere and ocean surface contributions from the top of atmosphere incident light field, we will be able to obtain the normalized water-leaving radiances, which can be related to water optical, biological, and biogeochemical properties.

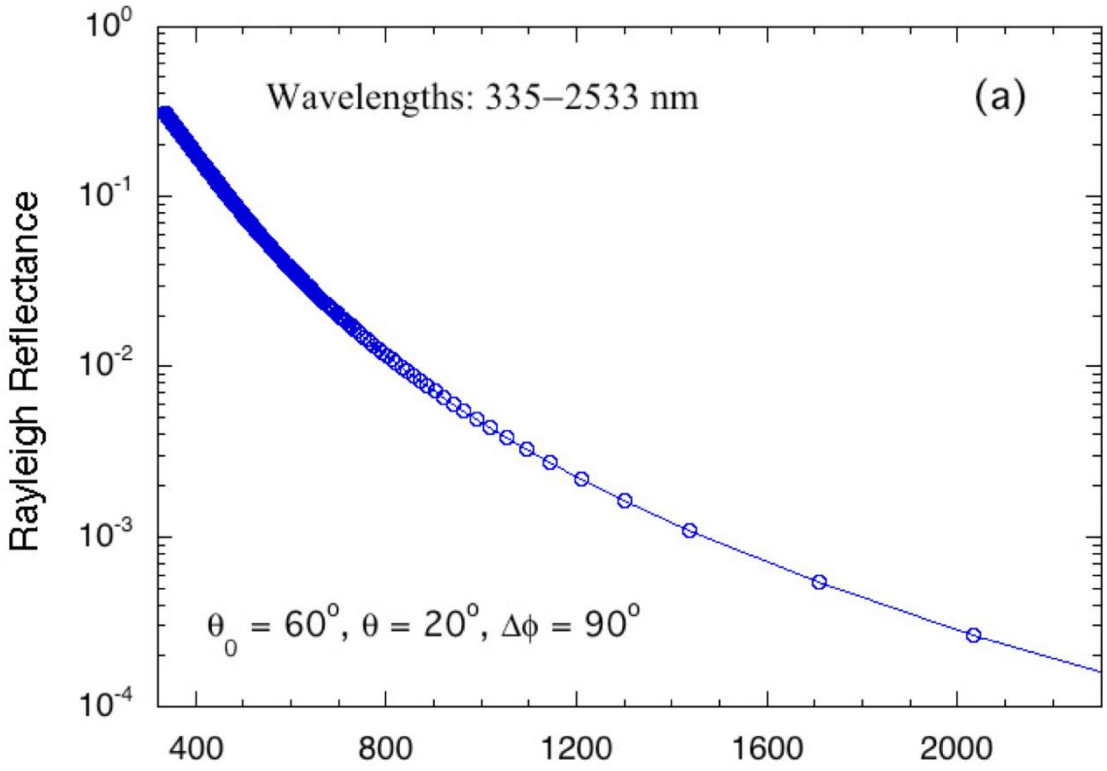

Figure 4. TOA Rayleigh-scattering radiances (F0(λ) = 1) for a case with solar- zenith angle of 60°, sensor-zenith angle of 20°, and relative-azimuth angle of 90° for (a) Rayleigh radiance as a function of the wavelength (Source: M. Wang, NOAA)

The apparent reflectance at the Top Of Atmosphere (TOA) is expressed as:

$$\rho^* = \rho^*_{na}\, T_g$$

where ρ_{na}^{*} is the signal ignoring the gaseous absorption and T_g the gaseous transmittance.

The spectral dependence of the Rayleigh optical thickness is well known. The optical thickness is proportional to the barometric pressure (P) at the ground surface. The geometry of the observation is described by the solar and viewing zenith angles and by the difference in the azimuth. Following Vermote et al. (1997), the Rayleigh contribution can be written as:

$$\rho_{na}^{*} = \rho_R + T_R(\mu_s)\frac{\rho_{aG}}{1-\rho_{aG}S_R}T_R(\mu_v)$$

where ρ_{na}^{*} is the apparent reflectance at TOA (corrected for gaseous absorption), ρ_R the Rayleigh reflectance, r_{aG} the aerosol-ground system reflectance, T_R (m_s) and T_R (m_v) the downward and upward Rayleigh transmittance respectively and S_R the spherical albedo relating to the molecules.

There are two basic assumptions contained in the second equation:

- On the vertical distribution: the molecular layer is put above the aerosol layer.
- On the bi-directionality of the radiances at the top of the aerosol layer. The BRR (bottom of Rayleigh) is assumed to be Lambertian.

Following the equation, we can easily correct for Rayleigh scattering to retrieve the reflectance above the aerosol-ground system. First, if we ignore the coupling between reflection and scattering:

$$\rho_{aG}^{c} = (\rho_{na}^{*} - \rho_R)/T_R(\mu_s)T_R(\mu_v)$$

And after correction of this term:

$$\rho_{aG} = \frac{\rho_{aG}^{c}}{1 + \rho_{aG}^{c} S_r}$$

For each band of the sensors, the Rayleigh optical thickness is estimated (ROT). After this, the Fourier series expansion of the Rayleigh phase function is calculated (Santer, 2010), and the Stoke vector is reduced to radiance or reflectance. At TOA the Rayleigh reflectance for the 3 Fourier terms is expressed as the product of the Rayleigh phase function by a term that depends on the geometry and on the ROT.

The Rayleigh transmittance applies both to the downward and the upward paths. It is the same function, it depends only on the zenith angle (Santer, 2010, Vermote et al., 1997):

$$T_R^{6S}(\tau R, \mu) = \frac{\left(\frac{2}{3} + \mu\right) + \left(\frac{2}{3} + \mu\right) e^{-\tau R/\mu}}{\left(\frac{4}{3} + \tau R\right)}$$

The transmittance is defined as the ratio between the downwelling total irradiance (direct and diffuse) at the surface to the incident solar irradiance at TOA.

The Rayleigh spherical albedo (SR) is defined as:

$$S_R(\tau R) = 1 - 2\int_0^1 T_R(\tau R, \mu)\mu d\mu$$

2. THE RAYLEIGH CORRECTION PROCESSOR

Rayleigh correction can be applied to:

- MERIS bands 1 to 15 (N1 format or MERIS 4th reprocessing format)
- OLCI L1B bands 1-21
- MSI L1C bands 1 to 9

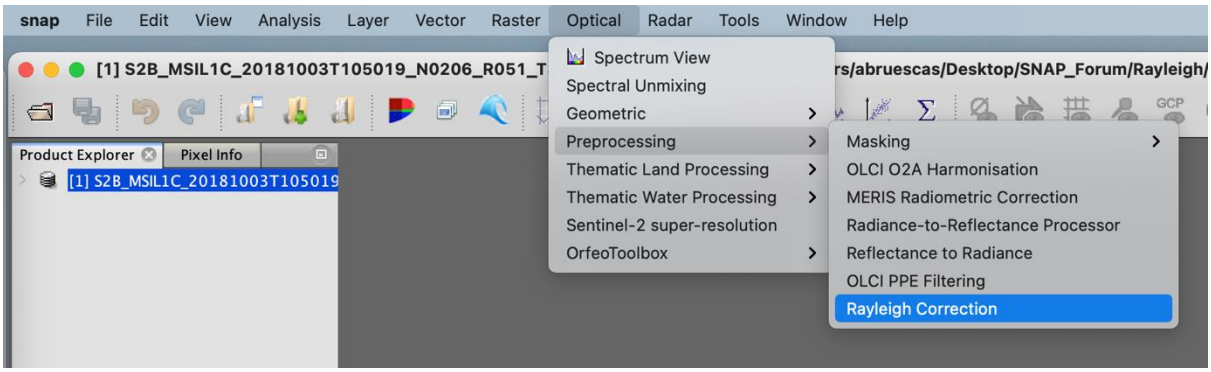

Figure 5. How to locate the Rayleigh correction processor

Five different outputs are common to the three sensors: Rayleigh optical thickness (ROT), Bottom of Rayleigh Reflectance (BRR), gaseous corrected TOA reflectance, TOA reflectance bands and air mass (the air mass term is written to the target product, otherwise is set to False).

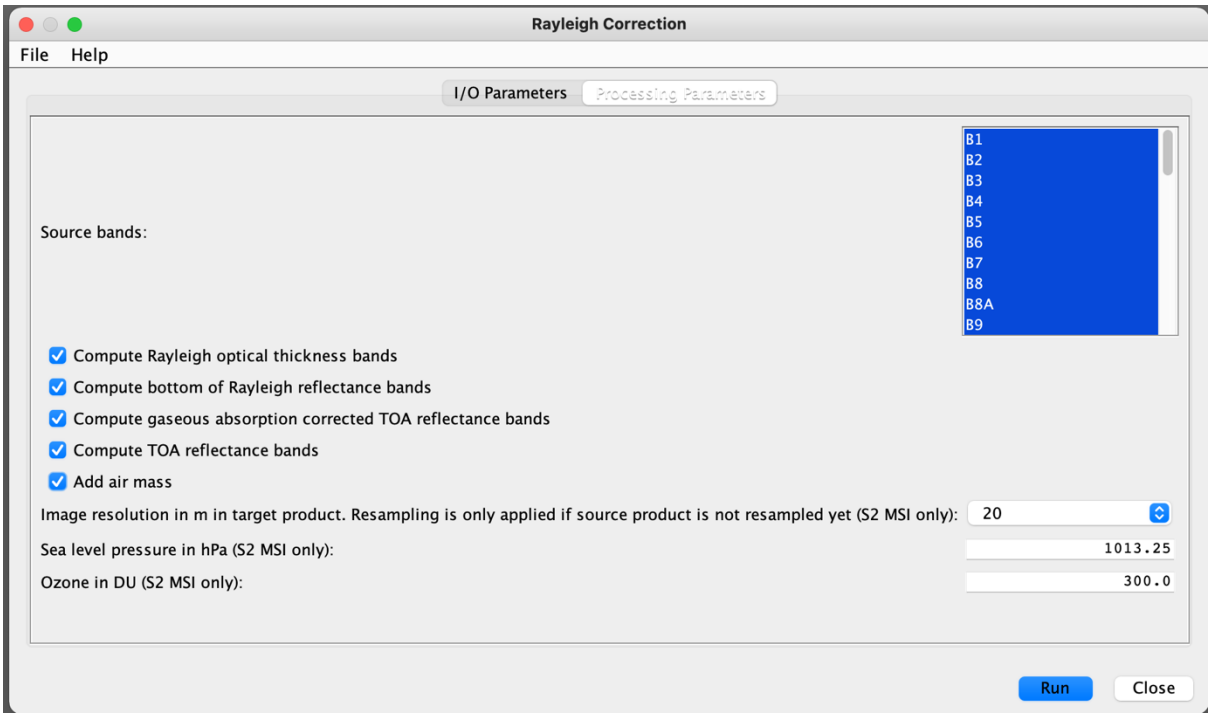

Figure 6. Optional outputs of the Rayleigh correction processor

2.1 RAYLEIGH OPTICAL THICKNESS

The Rayleigh correction processor for MERIS; OLCI and MSI starts with the calculation of the refractive index of dry air with 300 ppm CO_2 concentrations, following Peck and Reeder (1972):

$$n_{300} - 1\ x\ 10^8 = 8060.51 + \frac{2480990}{132.271 - \lambda^{-2}} + \frac{17455.7}{39.32957 - \lambda^{-2}}$$

and scaling for the desired CO2 concentrations,

$$n_{ratio} = 1 + 0.54(RayleighConstants.CO_2 - 0.0003)$$

being the *RayleighConstants.*CO_2 equal to 3.6 x 10^{-4}, which translates into a particle concentration of 360ppm.

The Rayleigh scattering cross section (cm2) of air is calculated by (Bodhaine et al, 1999):

$$\sigma = \frac{24\,\pi^3\,(n^2-1)^2}{\lambda^4 N_s^2 (n^2-2)^2} F_{air}$$

being F_{air}

$$F_{(air,CO_2)} = \frac{78.084F(N_2) + 20.946F(O_2) + 0.934\ x\ C_{CO_2} x\ 1.15}{78.084 + 20.946 + 0.934 + C_{CO_2}}$$

$$N_2 = 1.034 + 3.17\ x\ 10^{-4}\ \frac{1}{\lambda^2}$$

$$O_2 = 1.096 + 1.385\ x\ 10^{-3}\ \frac{1}{\lambda^2} + 1.44810^{-4}\ \frac{1}{\lambda^4}$$

$$Ns = 2.5469\ x\ 10^{19}$$

The Rayleigh optical depth is then calculated:

$$\tau_R(\lambda) = \sigma \frac{PA}{m_a\ g}$$

Being P the surface pressure, A the Avogrado's number (6.0221367E+23), m_a is the mean molecular weight of dry air calculated as 15.0556(CO_2) + 28.9595, and g is the acceleration of gravity, which is calculated having in account the latitude and the height above the sea level.

It is important to notice that the contribution of CO_2 to the Rayleigh optical depth of air is estimated as a function of wavelength. In the processor the true wavelength per band is

estimated by the sensors' spectral response function, and not the central wavelengths of their bands.

2.2 BOTTOM OF RAYLEIGH REFLECTANCE

The model of Rayleigh reflectance is stored in a LUT as a Fourier series with coefficients as functions of Rayleigh optical thickness (at wavelength), airmass, cosines of observation and sun zenith angle. From discrete angles in the LUT, values are interpolated to match the actual viewing and illumination geometry.

The Rayleigh reflectance is calculated as

$$\rho_R = \rho_{Rm}[0] + 2 * \rho_{Rm}[1] * \cos\Delta\varphi + 2 * \rho_{Rm}[2] * \cos(2 * \Delta\varphi)$$

with coefficients ρ_{Rm} and azimuth angle difference between sun and observation direction.

The Rayleigh transmittance in the direction of sun to surface tR_{θ_s} is calculated with the help of a quadratic polynomial (MERIS LUT):

$$tR_s = \frac{1}{\frac{4}{3} + \tau_r}\left(\frac{2}{3} + \cos\theta_s + \left(\frac{2}{3} - \cos\theta_s\right) * \exp\left(-\frac{\tau_r}{\cos\theta_s}\right)\right)$$

$$tR_{\theta_s} = \tau_{ray}[0] + \tau_{ray}[1] * tR_s + \tau_{ray}[2] * tR_s^2$$

And in the same way, the Rayleigh transmittance from the surface to the sensor is determined:

$$tR_v = \frac{1}{\frac{4}{3} + \tau_r}\left(\frac{2}{3} + \cos\theta_v + \left(\frac{2}{3} - \cos\theta_v\right) * \exp\left(-\frac{\tau_r}{\cos\theta_v}\right)\right)$$

$$tR_{\theta_v} = \tau_{ray}[0] + \tau_{ray}[1] * tR_v + \tau_{ray}[2] * tR_v^2$$

At top of atmosphere the Rayleigh corrected reflectance (including the absorption of ozone) can be expressed as the incident reflectance corrected for ozone absorption and the modelled Rayleigh reflectance, modified by the downward and upward transmittance:

$$\rho_{R_{corr}}^{TOA} = \frac{\rho_{ozone_{corr}}^{TOA} - \rho_R}{tR_{\theta_v} * tR_{\theta_s}}$$

The spherical factor accounts for the influence of the spherical albedo sa_R (LUT from MERIS, Zagolski et al, 2005) by

$$sphericalFactor = \frac{1}{1 + sa_R * \rho_{Rcorr}^{TOA}}$$

The top of aerosol reflectance is equal to the bottom of Rayleigh reflectance:

$$\rho_{BRR}(\lambda) = \rho_{Rcorr}^{TOA}(\lambda) * sphericalFactor$$

2.3 TOA Reflectance Bands

Top of atmosphere radiances are converted into reflectances with the help of the solar flux (included in MERIS and OLCI products) scaled by the sun zenith angle. The TOA reflectances are defined as:

$$\rho^{TOA}(\lambda) = \frac{radiance^{TOA}(\lambda) * \pi}{E_0(\lambda) * \cos\ \theta_s}$$

The S2-MSI product does not need this conversion, as the bands of measurements are natively provided as reflectances.

2.4 Air Mass

A simple measure of the path length of the radiation in the atmosphere, coming from the sun to the surface and leaving in the direction of the observing detector, is called air mass. It is defined as the sum of the inverse cosines of sun and view zenith angles:

$$airmass = \frac{1}{\cos\ \theta_s} + \frac{1}{\cos\theta_v}$$

The airmass minimum value is 2, when the sun is in zenith position $\theta_s = 0°$ and the observation takes place in nadir view. The radiation passes through the minimum extent of the atmosphere (in a simplified spherical model) two times. As sun and observation angles get larger (closer to the horizon), the path through the atmosphere gets longer, which is reflected in the air mass value.

3. EXAMPLE ON SENTINEL-2 MSI

The L1C MSI product consists of reflectance bands in multiple spatial resolutions (10, 20 and 60m). The Rayleigh Correction Processor can work with either this multiple resolution product or a resampled product. If the product is not resampled yet, the image resolution of the target product (in meter) has to be selected and resampling will automatically be executed before the Rayleigh correction procedure. While for MERIS and OLCI the information about sea level pressure and ozone is written in the tie point grids of the product and interpolated to each pixel, these parameters have to be set manually as a single value for the entire MSI scene. By default, the values are 1013.25 hPa and 300 DU respectively; and the spatial resolution is 20 m.

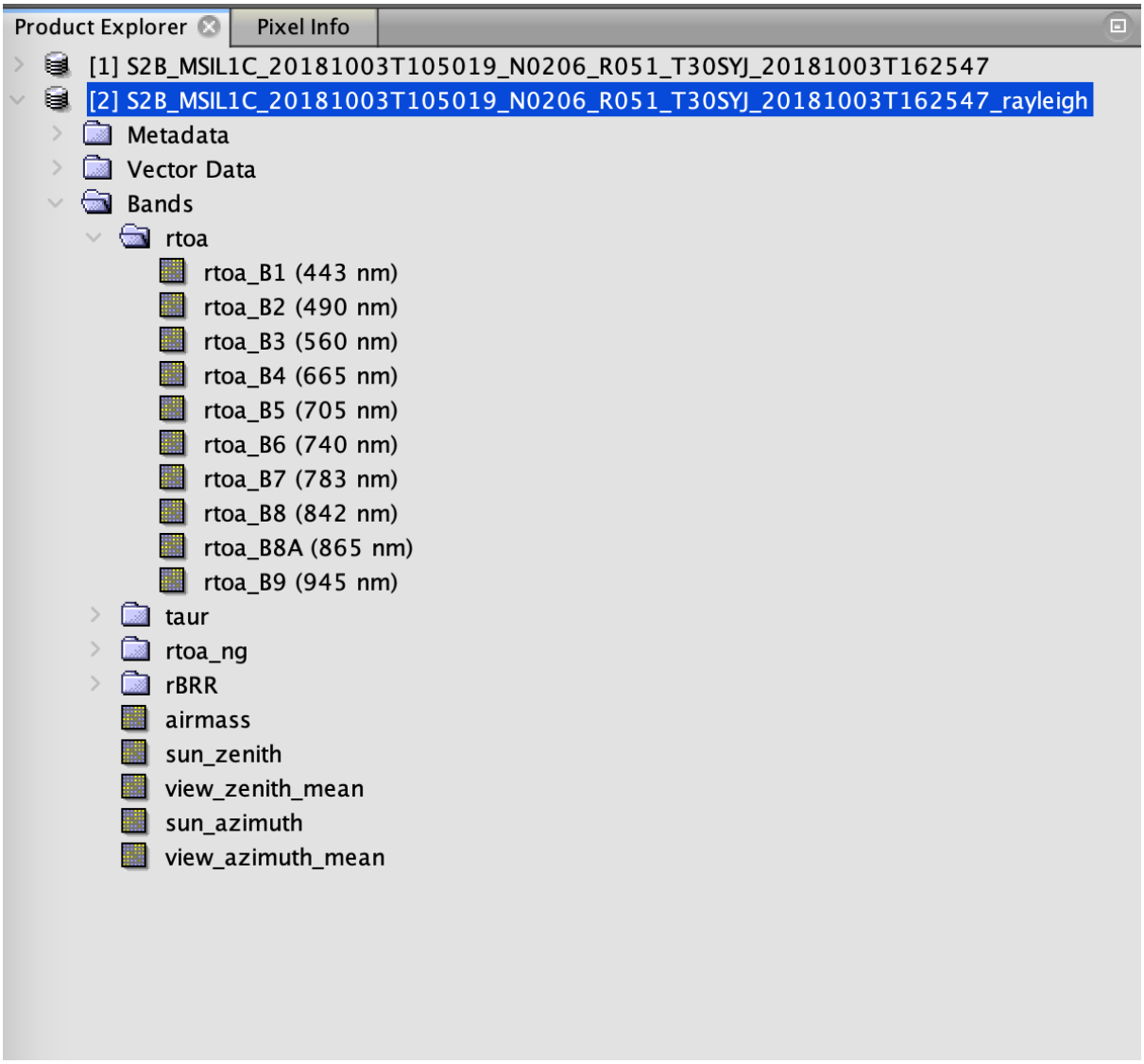

Figure 7. Bands generate after Rayleigh correction, with all options marked, on a S2-MSI scene

If we analyze the results using transects, we can observe the differences in the magnitude of TOA reflectance, the TOA reflectance including a correction for gas absorption and BRR products.

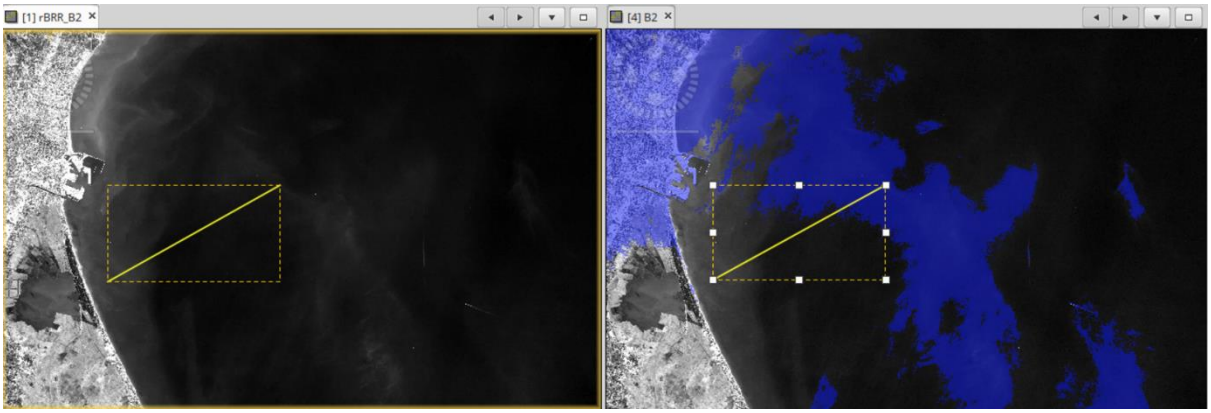

Figure 8. Comparison of products using a transect. B2 TOA reflectance on the right; B2 BRR on the left. The blue overlay shows the extent of cirrus clouds calculated with the pixel classification tool Idepix.

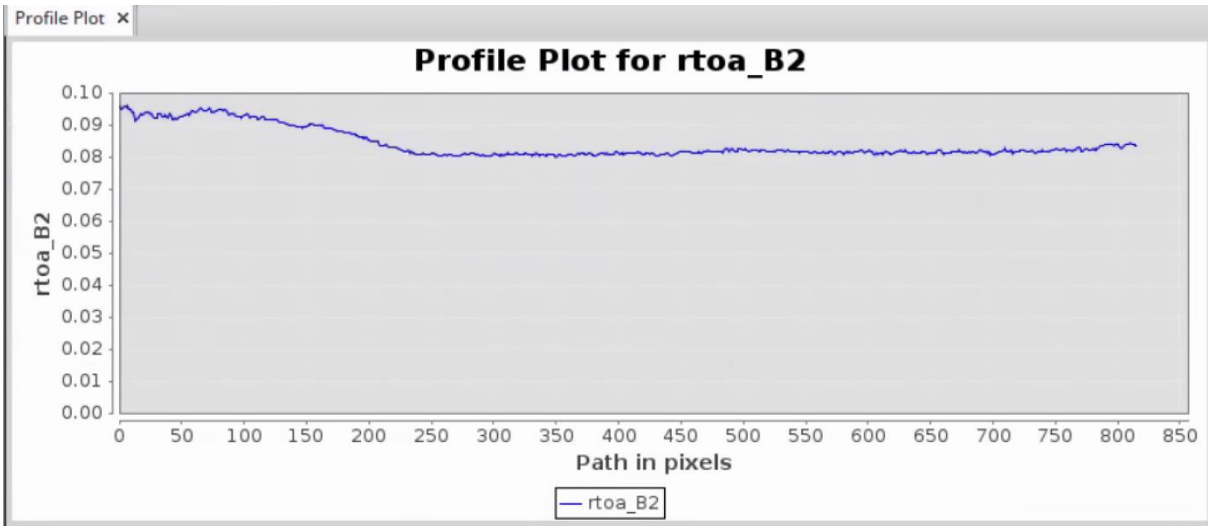

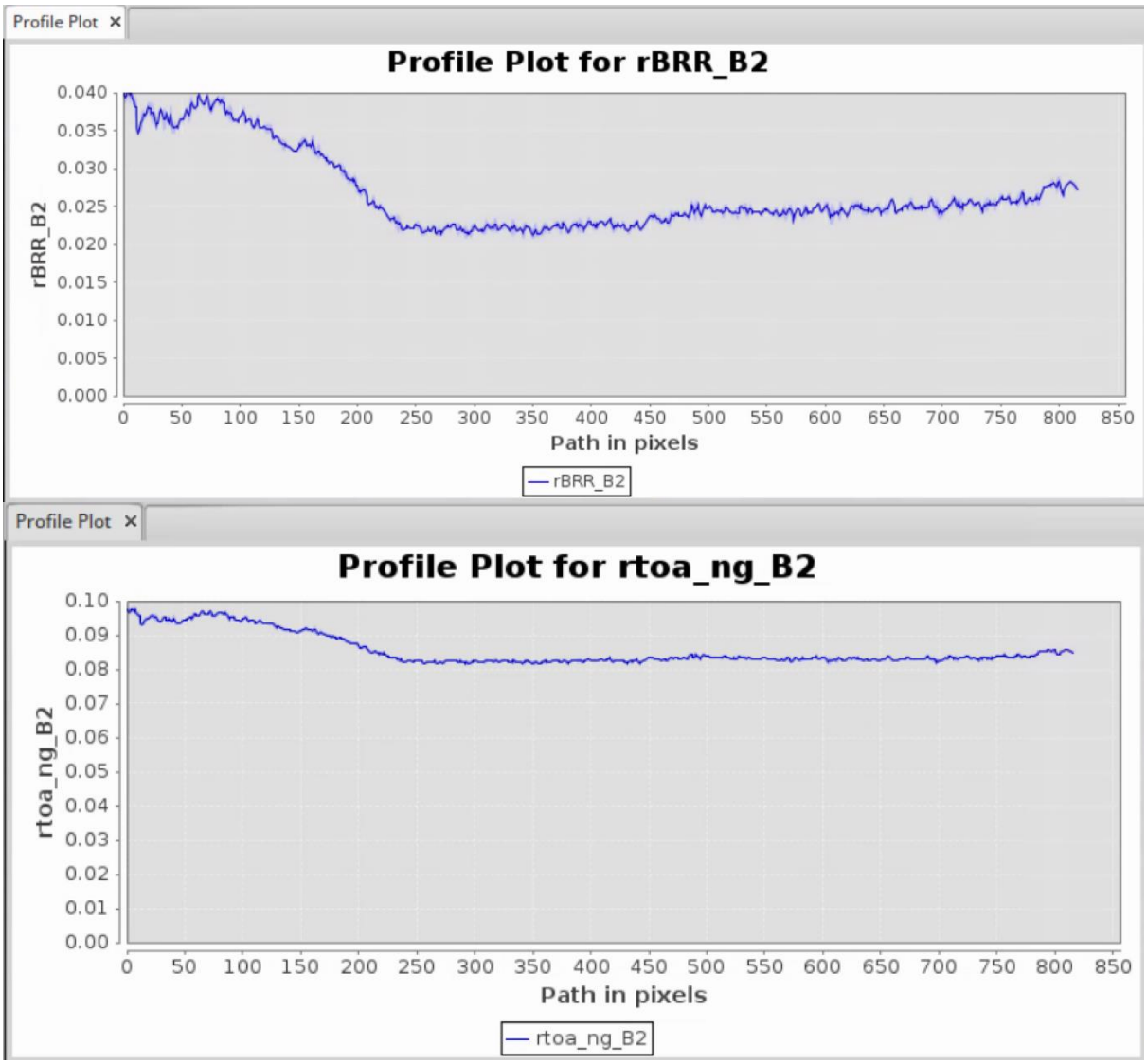

Figure 9. Differences among TOA reflectance, BRR and TOA after gaseous correction for the transect plot in Figure 9 (B2)

In Figure 10 we are able to observe the drop in the magnitude of the reflectance measured by the sensor after applying the Rayleigh correction to B2 (490nm), which is expected. These lower values can be observed through the transect (60% lower signal). In this profile we cannot see a big difference in shape or magnitude, if we compare the TOA reflectance and the TOA reflectance (rtoa_B2) after gaseous correction (rtoa_ng_B2). Figure 11 shows the same transect values for B6 (740 nm). The Rayleigh correction drops the magnitude again nearly to 50% of the TOA reflectance. As expected, the wavelength dependency of the Rayleigh scattering cross-section leads to a larger difference between reflectances at shorter wavelengths.

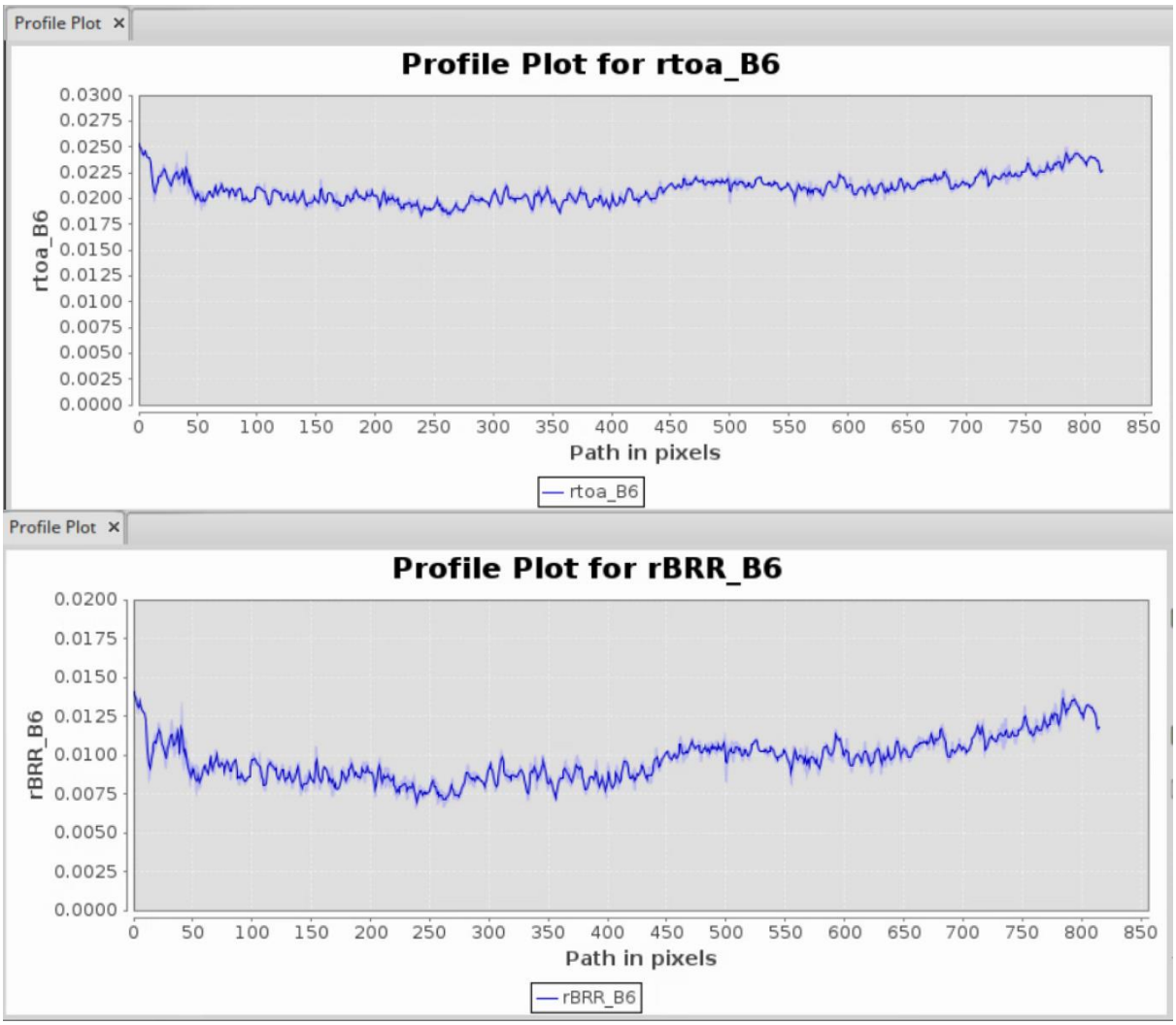

Figure 11. Differences among TOA reflectance, BRR and TOA after gaseous correction for the transect plot in Figure 9 (B6)

4. REFERENCES

- Bodhaine, B.A:, Wood, N.B., Dutton, E.G. and Slusser, J.R. (1999), On Rayleig Optical Depth Calculations, AMS, vol. 16, 1854-1861

- Bourg, L. (2009) MERIS Level 2 Detailed Processing Model. ACRI-ST, Document No. PO-TN-MEL-GS-0006, 15 July 2009.

- Liou, K. N.: An Introduction to Atmospheric Radiation, Academic Press, 525 B Street, Suite 1900, San Diego, California 92101-4495, USA,
- second edn., 2002.

- Santer et al. (2010) OLCI Level 2 Algorithm Theoretical Basis Document, Rayleigh correction over land, S3-L2-SD-03-C15-LISE-ATBD https://earth.esa.int/documents/247904/349589/OLCI_L2_Rayleigh_Correction_Land.pdf

- Wang M. (2016) Rayleigh radiance computations for satellite remote sensing: accounting for the effect of sensor spectral response function. Opt Express. 2016 May 30;24(11):12414-29. doi: 10.1364/OE.24.012414. PMID: 27410156.

- Zagolski F., Aubertin, G., J.F. Leroux, Péron G,.2005, Specification of the Scientific Contents of the MERIS Level 2 Auxiliary Data Product, BOMEN report, PO-RS-BOM-GS- 0002, 30 Nov 2005